FCRD Milestone Report: M21AF050901
Report on Mechanical Testing Studies on Large Scale Heat of an ODS Alloy
September 16, 2011

D.T. Hoelzer, M.A. Sokolov and T.S. Byun, ORNL
G.R. Odette, D. Klingensmith, D. Gragg, E. Stergar and K. Fields, UCSB

Objective

The objective of this study was to perform mechanical testing on large scale heats of the advanced ODS 14YWT alloy to investigate the effects of processing parameters on mechanical properties.

Background

Two heats of the advanced ODS 14YWT ferritic alloy referred to as 14YWT-SM11 and OW4 were produced for mechanical properties testing. The purpose for producing the two heats was to investigate the feasibility of using a large mild steel can for extruding ball milled powder and a modified ball milling condition with the CM08 attritor mill to reduce the contamination of the pre-alloyed Fe powder by O, C, and N interstitial atoms. Both of these factors were important to study since the knowledge obtained will be used to optimize the extrusions and hot isostatic pressing that will be used for consolidating the large 55 kg heat of 14YWT powder that will be ball milled by Zoz, GmbH, Germany at their pilot facility under subcontract with LANL and coordinated with ORNL.

The 14YWT-SM11 heat was the first heat that was produced with the larger capacity CM08 attritor mill. This heat was 3.0 kg (~6.6 lbs.) and was extruded at 850ºC in a 4 in. diameter mild steel can. The extruded bar was fabricated into plate that was ~1.0 cm thick. The chemical analysis results for this heat showed that significant contamination with O and N occurred during ball milling of the powder and remained high after extrusion as shown in Table 1. The next heat that was produced was 14YWT-PM1 using a modified ball milling condition designed to lower the contamination rate of interstitial O, C and N atoms. This heat was 2.4 kg (~5.3 lbs.) and was also extruded at 850ºC in a 4 in. diameter mild steel can. The chemical analysis of 14YWT-PM1 showed that the modified ball milling condition successfully reduced the contamination level of O, C and N as shown in Table 1. Unfortunately, since the atomized powder contained low O (Fe-14Cr-3W-0.4Ti-0.2Y-0.14O wt. %), the resulting O content was significantly too low to produce the desired high number density of nano-size oxide particles typical of the numerous smaller heats of 14YWT that have been produced. No mechanical properties testing were performed on 14YWT-PM1. Another experimental heat was then produced using the modified ball milling condition with the goal of elevating the O level while reducing the C and N levels. The 14YWT-PM2 heat consisted of 1.0 kg of powder with composition Fe-14Cr-3W-0.4Ti-0.2Y-0.14O (wt. %) that was ball milled with 0.3 % FeO powder to raise the O level. The chemical analysis shown in Table 1 demonstrated that this experimental procedure was successful in obtaining a high O concentration of 1352 wppm and low C and N levels of 140 wppm, respectively. The ball milled powder was then consolidated by Hot Isostatic Pressing (HIP) at UCSB and extrusion at ORNL. The OW4 heat was produced with 500 g of the ball

milled powder by HIPing at 1150ºC and 200 MPa and the 14YWT-PM2 heat was produced with the remaining 500 g of ball milled powder by extrusion at 850ºC.

Table 1. Chemical analysis results of ball milled powder and extruded heats of 14YWT.

Element	14YWT-SM11		14YWT-PM1		14YWT-PM2	
(wppm)	Milled Powder	Extrusion	Milled Powder	Extrusion	Milled Powder	Extrusion
O	2590	2470	447	337	1352	N/A
C	346	344	287	268	140	N/A
N	1911	3903	123	86	140	N/A

The microstructural characterization of 14YWT-SM11 and OW4 showed that both alloys contained a dispersion consisting of a high concentration ($>10^{23}$ m^{-3}) of 2-4 nm Ti- and Y-enriched oxide particles. The HIPed OW4 alloy contained a bimodal grain size structure with grain sizes of ~580 nm for ~10% and ~11 μm for 90% of the grains. The extruded 14YWT-SM11 contained a relatively uniform grain size structure, with most of the grains <500 nm in size and slightly elongated due to the extrusion and hot rolling procedures.

Results and Discussion of Mechanical Properties Testing

The mechanical properties tests that have been conducted consisted of Vickers Hardness and tensile tests at room temperature on 14YWT-SM11 and OW4; tensile tests over a temperature range of -100ºC to 800ºC on 14YWT-SM11; fracture toughness tests at different temperatures on 14YWT-SM11 and OW4 and strain rate jump tests at 750ºC on OW4.

Tensile and Hardness Properties

The Vickers Hardness Number (VHN) was measured at room temperature on both 14YWT-SM11 and OW4. The VHN obtained for 14YWT-SM11 was 725 +/- 17.6, which was very high and corresponded to an estimated strength of 2.37 +/- 0.06 GPa. This value obtained for 14YWT-SM11 represented the highest VHN compared to all previous heats of 14YWT that have been produced. For OW4, the room temperature hardness was found to be 368 +/- 4 VHN, with an estimated strength of 1.20 +/- 0.01 GPa. This hardness was considerably lower than that measured for 14YWT-SM11.

The results of the tensile tests conducted on 14YWT-SM11 and OW4 at room temperature were similar to the hardness data. The tensile curves obtained from tensile tests using a strain rate of ~2 x 10^{-3} s^{-1} are shown in Figure 1. Overall, the 14YWT-SM11 had a significantly higher strength but less ductility compared to OW4. The yield stress (σ_{ys}) and ultimate tensile strength (σ_{uts}) for 14YWT-SM11 were 1.46 GPa and 1.862 GPa, respectively, compared to σ_{ys} = 0.86 GPa and σ_{uts} = 1.02 GPa, respectively for OW4. The σ_{uts} values for both alloys are lower than the estimated strength calculated with the VHN by ~15-20%. The uniform (UE) and total (TE) elongation measured for 14YWT-SM11 were 3.8% and 7.6%, respectively. These values are much lower than that measured for OW4, which were UE = 9.5% and TE = 17.6% at room
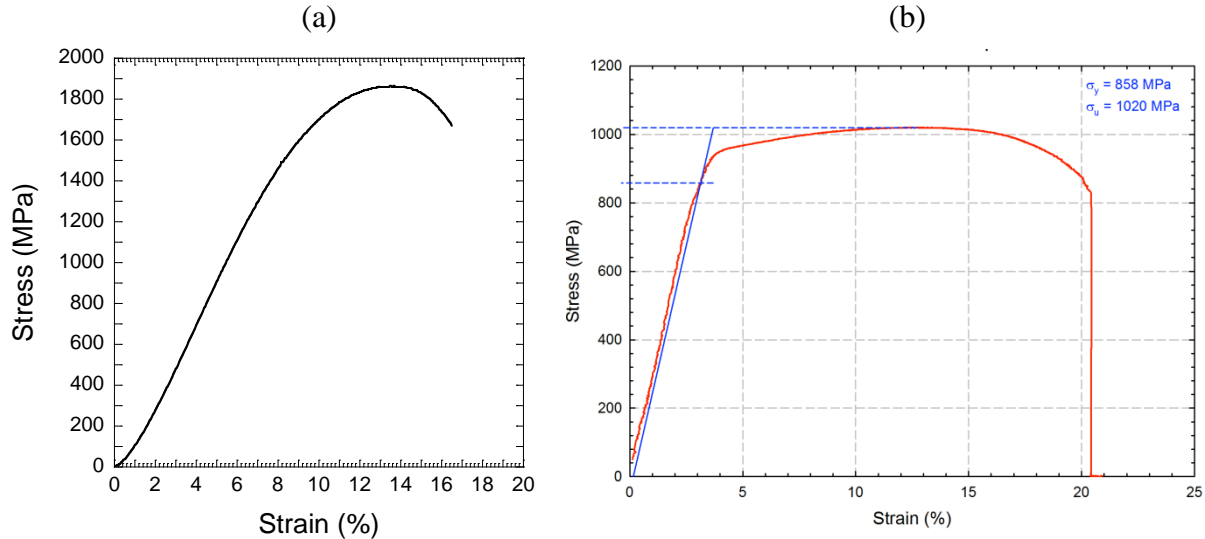
Figure 1. Tensile curves conducted at room temperature using strain rate of ~2 x 10^{-3} s^{-1}. (a) 14YWT-SM11 and (b) OW4.

temperature. These results are consistent with the commonly observed trend showing that as the ductility decreases, the strength of an alloy increases and vice versa. The significantly higher strength obtained for 14YWT-SM11 was in part due to the more uniform distribution of ultra-fine grains compared to OW4. In addition, the higher N and O level in 14YWT-SM11 most likely also contributed to the higher strength. Microstructural analysis of previous heats of 14YWT containing elevated N levels showed that N segregation to grain boundaries can occur, which may increase the contribution of the ultra-fine grain size to Hall-Petch strengthening. However, the exact strengthening mechanism is not fully understood.

Tensile tests were performed on 14YWT-SM11 at -100ºC, 25ºC, 500ºC and 800ºC to compare with the tensile data obtained from previous heats of 14YWT. This comparison is shown in Figure 2. Interestingly the σ_{uts} for 14YWT-SM11 was consistently the highest except at 800ºC. The σ_{ys} varied considerably over the temperature range, but was the lowest value at room temperature and at 800ºC. At temperatures below 500ºC, the work hardening capacity of 14YWT-SM11 was better than that of the SM4, SM6 and SM10 heats of 14TYWT. In all tests, the specimen experienced necking due to plastic deformation instability after reaching uniform strain. This observation indicated that some ductile deformation was operative during the tests, even the one at -100ºC. Further tensile tests will be conducted on 14YWT-SM11 to obtain a better understanding of this tensile properties behavior.

Fracture Properties

The fracture toughness tests were conducted in accordance with the ASTM E 1921-02 [1] Standard Test Method for Determination of Reference Temperature, T_o, for Ferritic Steels in the Transition Range, with a computer-controlled test and data acquisition system. The small (12.5 mm in diameter with thickness of 2 mm) disk compact [DC(T)] specimens were fatigue precracked to a ratio of the crack length to specimen width (a/W) of about 0.5. The unloading
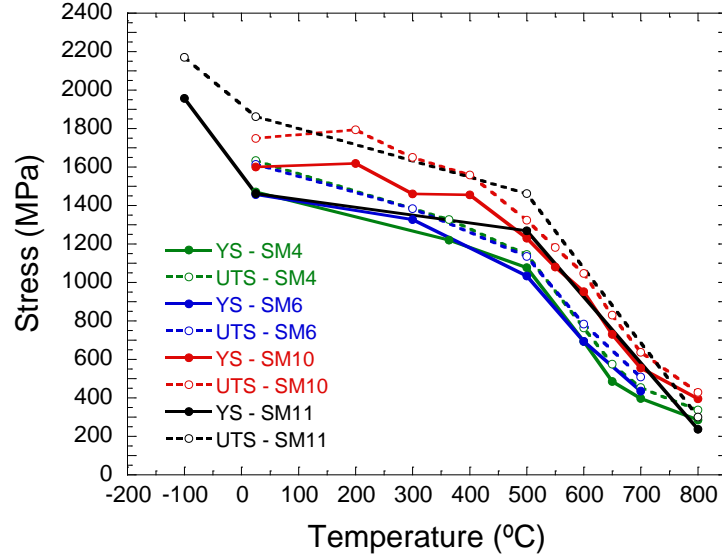
Figure 2. Comparison of the yield stress and ultimate tensile stress for 14YWT-SM11 and previous 14YWT heats (SM4, SM6 and SM10).

compliance method used for measuring the J-integral with these specimens is outlined in Ref. [2]. Specimens were tested in the laboratory on a 98-kN (22-kip) capacity servohydraulic machine. All tests were conducted in strain control, with an outboard clip gage having a central flexural beam that was instrumented with four strain gages in a full-bridge configuration. The broken specimens were examined with a calibrated measuring optical microscope to determine the initial and final crack lengths.

Values of J-integral at cleavage instability, J_c, were converted to their equivalent values in terms of stress intensity K_{Jc} by the following equation [1]:

$$K_{Jc} = \sqrt{J_c \frac{E}{1-v^2}} \tag{1}$$

where E is Young's modulus and v is Poisson's ratio.

It was assumed that the transition fracture toughness of 14YWT alloy complies with the master curve concept. After that, all K_{Jc} data were converted to 1T equivalence, $K_{Jc(1T)}$, using the size adjustment procedure of ASTM Standard E1921 [1]:

$$K_{Jc(1T)} = 20 + \left[K_{Jc(x)} - 20\right] \cdot \left(\frac{B_x}{B_{1T}}\right)^{1/4} \tag{2}$$

where $K_{Jc(x)}$ = measured K_{Jc} value,
B_x = gross thickness of test specimen,
B_{1T} = gross thickness of 1T C(T) specimen.

The reference fracture toughness transition temperature, T_o, was determined using the multi-temperature equation from E1921 [1]:

$$\sum_{i=1}^{N} \delta_i \frac{\exp\left[0.019\left(T_i - T_o\right)\right]}{11 + 77\exp\left[0.019\left(T_i - T_o\right)\right]} - \sum_{i=1}^{N} \frac{\left(K_{Jc(i)} - 20\right)^4 \exp\left[0.019\left(T_i - T_o\right)\right]}{\left\{11 + 77\exp\left[0.019\left(T_i - T_o\right)\right]\right\}^5} = 0 \qquad (3)$$

where $\delta_i = 1.0$ if the datum is valid or zero if datum is invalid (in this study all data were ASTM E1921 valid because of extremely high strength of this alloy, T_i = test temperature corresponding to $K_{Jc(i)}$.

The fracture toughness of SM-11 heat of 14YWT alloy was examined in two orientations, L-T and T-L. It is well know now that fracture toughness of this alloy has very strong orientational dependence. For specimens of L-T orientation, the tension is applied in longitudinal, extrusion (L) orientation, while crack propagates in transverse (T) orientation. Typically, this is the toughest orientation. For specimens in T-L orientation, the tension is applied in T orientation and crack propagates in L orientation. Typically, the T-L orientation is the weakest, from fracture toughness point of view, orientation. The test results are summarized in Table 2.

Table 2. Fracture toughness data of 14YWT-SM11.

Orientation	Specimen ID	Test Temp., ^{o}C	K_{Jc}, MPa√m	$K_{Jc(1T)}$, MPa√m
T-L	D00	25	66.8	44.8
T-L	D10	25	51.5	36.7
T-L	D06	25	48.2	34.9
T-L	D02	-50	34.5	27.7
T-L	D08	-50	63.7	43.1
L-T	D20	25	89.5	56.8
L-T	D18	25	146.1	86.8
L-T	D22	25	157.9	93.1
L-T	D23	-50	58.4	40.3
L-T	D13	-50	46.1	33.8

Figure 3 illustrates the fracture toughness of this heat in two orientations. In addition to transition fracture toughness tests, one specimen in L-T orientation was tested at 100°C to estimate ductile fracture toughness. It failed in ductile instability exhibiting toughness of 134 MPa√m at ductile instability. This result shows that this alloy has very little or none (like for heat SM-11) resistance to stable crack growth. It appears that heat SM-11 has higher transition fracture toughness temperature, T_o, compared to other heats of this alloy. Yet, the fracture toughness of this heat in the weakest orientation is similar to fracture toughness of alloy 12YWT [3] in the strongest orientation, see Figure 4. While the difference between T_o in T-L and L-T remains relatively high (63°C), this difference is the lowest observed for this alloy.
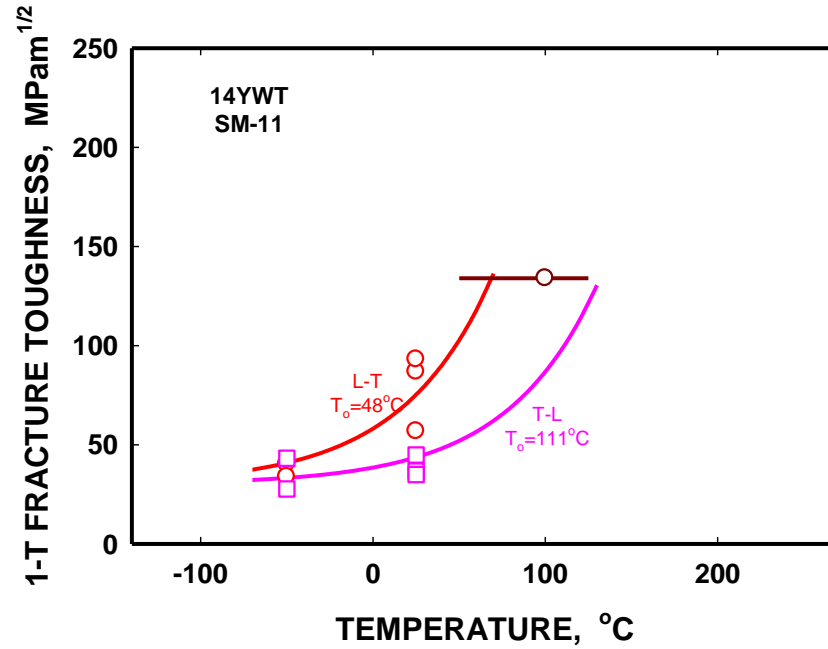
Figure 3. Fracture toughness of the 14YWT-SM11 alloy in the L-T and T-L orientations.
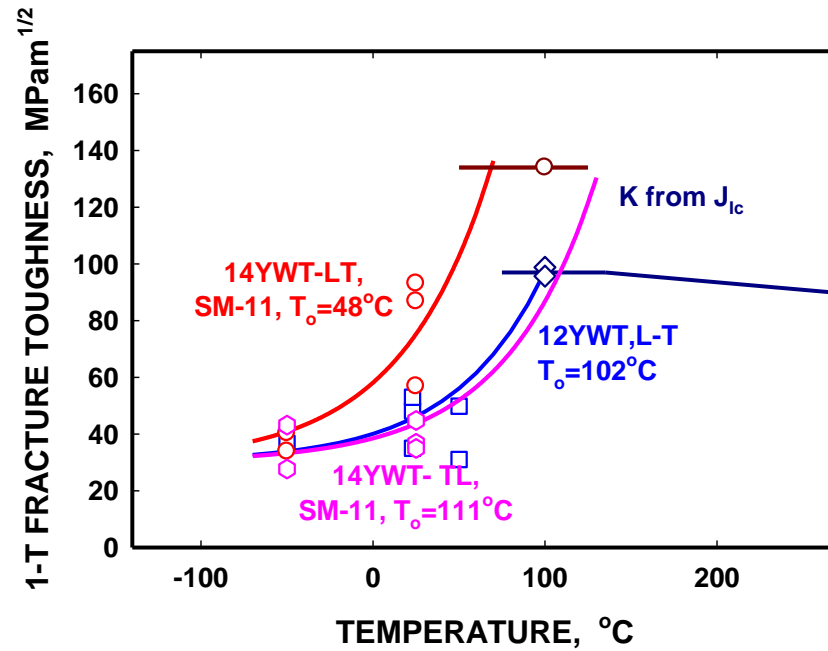

Figure 4. Fracture toughness of the 14YWT-SM11 alloy in two orientations compared to fracture toughness of 12YWT alloy [3].

The fracture toughness tests conducted on OW4 used mini-bend bars to investigate the fracture toughness transition temperature and the fracture toughness from room temperature to 600°C. The results of the fracture toughness tests for OW4 are shown in Figure 5. The fracture toughness transition temperature for OW4 was above room temperature and was ~100°C, but

further testing at temperatures higher than 150ºC are required to more accurately determine the transition temperature. The lowest fracture toughness value was 27.4 MPa√m at room temperature and the highest fracture toughness value was measured at 150ºC to be 70.2 MPa√m. The fracture mode at room temperature was determined to be linear elastic cleavage fracture with small regions of tearing. The start of elastic-plastic fracture regime with predominantly cleavage (quasi-cleavage) fracture occurred at 100ºC. Small regions of tearing were also observed on the fracture surface. At 150ºC, fracture occurred by elastic-plastic cleavage pop-ins followed by ductile tearing crack extension, which resulted in the highest fracture toughness for OW4.

The fracture toughness test that was conducted at 600ºC showed that it decreased to 53 MPam$^{1/2}$ from the high of 70.2 MPa√m at 150ºC as shown in Figure 5. This result showing a decrease in fracture toughness as temperature increases was first observed in the fracture toughness study of 14YWT [4]. In this study, the fracture toughness of 14YWT (SM10 heat) was above 140 MPa√m at low temperatures, room temperature (RT) and 200 °C, but decreased to a low fracture toughness range of 52–82 MPa√m at higher temperatures up to 700 °C. The fractography results indicated that the ultra-fine grain structure of 14YWT produced shallow plasticity layers at high temperatures and a low-ductility grain boundary debonding mechanism occurred at 700 °C. These results indicate that investigation of fabrication methods for 14YWT and other ODS alloys are required in order to improve resistance to cracking at elevated temperatures.
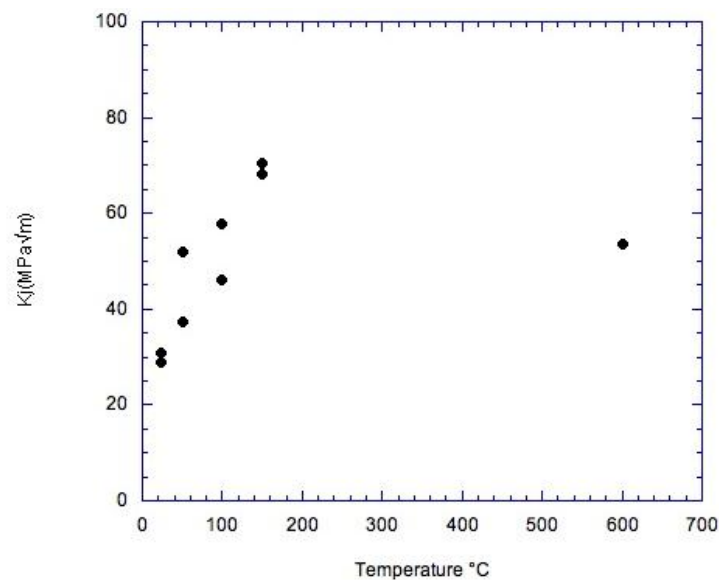

Figure 5. Fracture toughness results from room temperature to 600ºC measured for OW4.

Creep Properties

A series of strain rate jump tensile tests were conducted on OW4 to investigate the creep behavior at 750ºC. In these tests, the tensile specimens were tested in air on a MTS load frame at 750ºC starting at a low imposed strain rate, ε̇, usually 10^{-7} s^{-1}, and holding until a constant steady state stress level was reached. The ε̇ was then increased typically by an order of magnitude and held until the steady state stress was reached once again. A sequence of strain rate jump tests

were obtained in order to characterize the stress as a function of temperature and strain rate which were then used for investigating the creep behavior of OW4.

The strain rate jump test results compiled from several tests on OW4 are shown in Figure 6. Consistent with bcc alloys, such as ODS OW4, the σ_{ys} and σ_{uts} both increased as the strain rate was increased. The values of σ_{uts} obtained from the strain rate jump test compilation were then used to obtain the Larson Miller Parameter (LMP) that is shown Figure 6. The LMP is a parametric model that assumes the steady state creep regime follows a power law creep mechanism. The time-temperature relationship for predicting rupture and creep stresses is:

$$P_{L\text{-}M} = T(C + \log t)$$

where $P_{L\text{-}M}$ is the Larson-Miller parameter, T is the absolute creep test temperature, C is the Larson-Miller constant, and t is time to either creep rupture or to a given creep strain rate level. For the data obtained from the strain rate jump tests, the $P_{L\text{-}M}$ was determined by substituting the inverse minimum creep rate for time, allowing the prediction of creep rates instead of lifetimes. The Larson-Miller Plot for the inverse minimum creep rate (C = 30) data for OW4 as well as LMP data obtained for MA957 from strain rate jump tests [5] is shown in Figure 7. The results showed that the creep performance of OW4 was similar to that of MA957 at 750°C. These results also indicated that strain rate jump tests can be used to obtain important creep parameters in a short period of time.
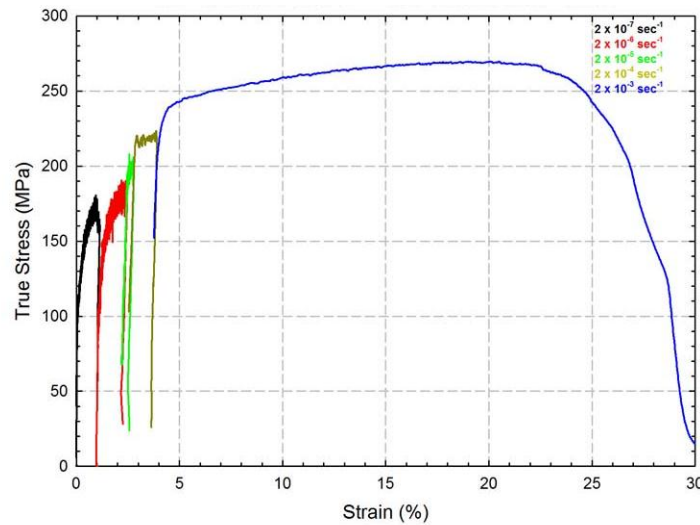

Figure 6. Strain rate jump test conducted on OW4 at 750°C.

A total of 6 creep specimens had been fabricated from 14YWT-SM11. The creep specimens are 1.65 in. long cylindrical shaped specimens that were prepared with threaded grips, extensometer grooves and gage that was 0.4 in. long and 0.113 in. diameter. These specimens were planned to be tested using the MTS load frame in constant stress control with up to 3 stresses at temperatures of 500°C and 700°C. Unfortunately, there currently has not been any available time on the MTS load frame at ORNL due to the very busy schedule for testing specimens from other programs including HFIR surveillance.
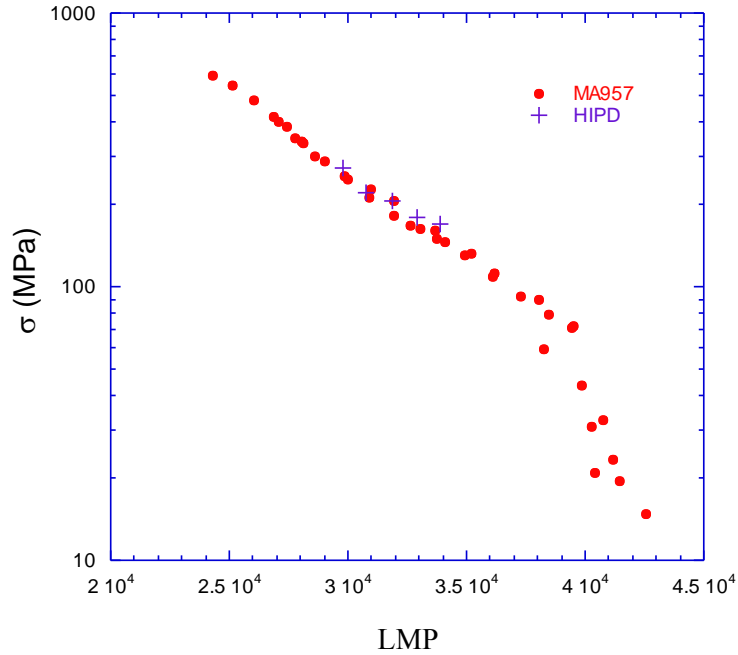
Figure 7. Comparison of strain rate jump test results obtained for OW4 at 750ºC with data for MA957.

Summary

Mechanical properties tests were conducted on two heats of the advanced ODS 14YWT ferritic alloy: the 14YWT-SM11 was produced by extrusion at ORNL and OW4 was produced by HIP at UCSB. The 14YWT-SM11 showed very high tensile strength compared to OW4, but showed less ductility as a result. The fracture toughness transition temperature of 14YWT-SM11 was determined in two orientations and showed $T_0 = 48ºC$ in the favorably strong L-T direction while shifting by 63ºC to $T_0 = 111ºC$ in the weaker T-L direction. The fracture toughness transition temperature for OW4 was not determined but appeared to be within the range observed for 14YWT-SM11. The fracture toughness of 14YWT-SM11 at room temperature was 86.8 MPa√m and 93.1 MPa√m, which was much higher than that of OW4 (27.4 MPa√m). The strain rate jump tests conducted on OW4 indicated that the creep properties were similar to MA957 at 750ºC.

Future Work Plan

The high temperature fracture toughness data obtained for 14YWT-SM11 will be processed to compare with results obtained from the study on 14YWT-SM11 and OW4. Creep tests using the fabricated tensile specimens of 14YWT-SM11 will be performed at 500 ºC and 700ºC with high stresses. Additional tensile specimens will be fabricated with the gage parallel and normal to the extrusion axis and tested over the temperature range of -100 ºC to 800 ºC to investigate the role of grain structure anisotropy on the tensile strength and tensile fracture behavior.

Reference

(1) D.J. Alexander, "Fracture Toughness Measurements with Subsize Disk Compact Specimens," *Small Specimen Test Techniques Applied to Nuclear Reactor Vessel Thermal Annealing and Plant Life Extension, ASTM STP 1204*, W.R. Corwin, F.M. Haggag, and W.L. Server, Eds., ASTM, Philadelphia, 1993, pp.130-142.

(2) Standard Test Method for Determination of Reference Temperature, T_o, for Ferritic Steels in the Transition Range, Designation E 1921-02, Annual Book of ASTM Standards, Vol. 03.01.

(3) M.A. Sokolov , D.T. Hoelzer, R.E. Stoller, D.A. McClintock, Journal of Nuclear Materials Vol. 367–370, (2007), p. 213.

(4) T.S. Byun, J.H. Kim and D.T. Hoelzer, Journal of Nuclear Materials, Vol. 407, Issue 2, (2010), p. 78.

(5) M.C. Salston and G.R. Odette, Fusion Semiannual Report, DOE/ER-0313/44, (2010), p. 62.